

Dynamical correlation energy of metals in large basis sets from downfolding and composite approaches

James M. Callahan,¹ Malte F. Lange,¹ and Timothy C. Berkelbach^{1,2}

¹*Department of Chemistry, Columbia University, New York, New York 10027 USA*

²*Center for Computational Quantum Physics, Flatiron Institute, New York, New York 10010 USA^{a)}*

(Dated: 11 March 2021)

Coupled-cluster theory with single and double excitations (CCSD) is a promising *ab initio* method for the electronic structure of three-dimensional metals, for which second-order perturbation theory (MP2) diverges in the thermodynamic limit. However, due to the high cost and poor convergence of CCSD with respect to basis size, applying CCSD to periodic systems often leads to large basis set errors. In a common “composite” method, MP2 is used to recover the missing dynamical correlation energy through a focal-point correction, but the inadequacy of MP2 for metals raises questions about this approach. Here we describe how high-energy excitations treated by MP2 can be “downfolded” into a low-energy active space to be treated by CCSD. Comparing how the composite and downfolding approaches perform for the uniform electron gas, we find that the latter converges more quickly with respect to the basis set size. Nonetheless, the composite approach is surprisingly accurate because it removes the problematic MP2 treatment of double excitations near the Fermi surface. Using the method to estimate the CCSD correlation energy in the combined complete basis set and thermodynamic limits, we find CCSD recovers over 90% of the exact correlation energy at $r_s = 4$. We also test the composite and downfolding approaches with the random-phase approximation used in place of MP2, yielding a method that is more effective but more expensive.

INTRODUCTION

Ground-state electronic properties of metallic solids have traditionally been computed using density functional theory (DFT),^{1–4} which is partially justified by the fact that many popular functionals are parameterized by numerically exact results on the uniform electron gas (UEG).^{5–8} In recent years, interest has grown around the application of *ab initio*, wavefunction-based electronic structure techniques for condensed-phase systems,^{9–16} since they do not suffer from uncontrolled errors inherent to the DFT exchange-correlation functional.^{6,17,18} Promising methods in this direction include the random-phase approximation (RPA)^{16,19,20} and coupled-cluster theory.^{21–26} Importantly, both of these methods preclude the well-known divergences of finite-order perturbation theories, such as second-order Møller-Plesset perturbation theory (MP2), via an infinite-order resummation.^{27–31}

Although coupled-cluster theory has been successfully applied to an increasing number of atomistic semiconductors and insulators,^{14,15,32–37} its applicability for metals has been primarily focused around the UEG, also known as jellium.^{29,38–45} Despite their reasonable accuracy, these calculations have demonstrated the typical slow convergence of the correlation energy as a function of the number of virtual (unoccupied) orbitals included.^{11,40,46,47} This slow convergence is especially problematic because of the high cost of coupled-cluster calculations with large basis sets. For example, coupled-cluster theory with single and double excitations (CCSD) has a computational cost that scales as $O(N^2M^4)$, where N and M are the number of electrons and basis functions respectively. To date, results near the complete basis set (CBS) limit have been primarily computed via the extrapolation of results obtained with a finite, increasing number

of basis functions,^{24,40,45} although explicitly correlated⁴⁸ and transcorrelated^{49,50} methods provide promising alternative approaches.

Composite methods (sometimes called focal point methods) are a simple, alternative class of approaches for recovering dynamical correlation within large basis sets.^{51–53} A common composite scheme combines the results of high-level and low-level theories using three calculations. For example, using CCSD as the high-level theory and MP2 as a low-level theory, the CCSD correlation energy in a large basis is approximated as

$$E_{\text{CCSD}}(M) \approx E_{\text{CCSD}}(M_{\text{act}}) + E_{\text{MP2}}(M) - E_{\text{MP2}}(M_{\text{act}}) \quad (1)$$

where $M_{\text{act}} < M$ is the number of “active” basis functions. Refs. 54 and 55 provide a similar but more sophisticated CCSD/MP2 composite method, based on an analysis of the basis set convergence of various diagrammatic contributions to the correlation energy. While such CCSD/MP2 composite approaches have been applied successfully to a number of semiconductors and insulators,^{36,54,56,57} their applicability to metals is questionable because of the failures of MP2 theory. One goal of this work is to test the composite CCSD/MP2 approach for metals.

A more theoretically satisfying approach would be to perform a single calculation where low-energy excitations near the Fermi surface are treated with CCSD and are coupled to high-energy excitations treated with MP2. This particular approach, which is similar to tailored CC⁵⁸ and the broader class of active-space CC methods,^{59–63} has variously been called CC/PT,⁶⁴ CCSD-MP2,⁶⁵ and multilevel CC.^{66,67} Two of us (M.F.L. and T.C.B.) recently tested this method for a few simple atomistic semiconductors and insulators,⁵⁶ and here we aim to assess its performance for metals, where the differences between CCSD and MP2 are more striking. Since the effects of the frozen high-energy MP2 amplitudes are folded down onto the low-energy CCSD amplitudes (see below), we

^{a)}Electronic mail: tim.berkelbach@gmail.com

refer to this method as a “downfolding” approach. In principle, this downfolding CCSD/MP2 method should provide a distinct advantage over the conceptually simpler composite approach, as downfolding does not include the MP2 treatment of low-energy excitations that are responsible for divergence in the thermodynamic limit (TDL). After providing theoretical details of these two methods, we compare their performance for the UEG at a fixed number of electrons and in the TDL. Before concluding, we also examine the straightforward use of the RPA in place of MP2.

THEORY

Here we briefly review the theory underlying the downfolding and composite approaches. The N occupied spin-orbitals are indexed by i, j, k, l ; the $(M - N)$ virtual orbitals by a, b, c, d ; and the M general orbitals by p, q, r, s . The MP2 and coupled-cluster with double excitations (CCD) correlation energies are given by

$$E_c = \frac{1}{4} \sum_{ijab} t_{ij}^{ab} \langle ij || ab \rangle \quad (2)$$

where t_{ij}^{ab} are amplitudes of the double excitation operator $T_2 = \frac{1}{4} \sum_{ijab} t_{ij}^{ab} a_a^\dagger a_b^\dagger a_j a_i$ and $\langle pq || rs \rangle$ are antisymmetrized two-electron repulsion integrals; contributions from single excitations vanish because the UEG has no capacity for orbital relaxation by symmetry. At lowest order in perturbation theory,

$$t_{ij}^{ab} = \frac{\langle ab || ij \rangle}{\varepsilon_i + \varepsilon_j - \varepsilon_a - \varepsilon_b}, \quad (3)$$

and Eq. (2) gives the MP2 correlation energy. The high density of states at the Fermi surface and the long-ranged nature of the Coulomb potential are together responsible for the divergence of MP2 in the TDL. By contrast, the CCD amplitudes solve a system of nonlinear equations

$$0 = \langle \Phi | e^{-T_2} H e^{T_2} | \Phi \rangle, \quad (4)$$

where H is the electronic Hamiltonian. A standard approach for reaching the CBS limit is to perform a series of calculations with increasing M and use a M^{-1} extrapolation.

In both the composite and downfolding approaches, we partition the orbitals into a set of M_{act} active orbitals, composed of all occupied orbitals and the low-energy virtual orbitals, and a set of $(M - M_{\text{act}})$ frozen (inactive) orbitals, composed of the high-energy virtual orbitals. In principle, occupied orbitals can also be partitioned, but typically they do not significantly contribute to the computational cost. In the composite CCD/MP2 approach, the correlation energy is calculated according to Eq. (1). Importantly for metals, the low-energy active space double excitations are treated by CCD and not by MP2, so we expect the method to be well-behaved in the thermodynamic limit.

In the downfolding CCD/MP2 approach, the double excitation operator T_2 is partitioned into internal excitations fully

contained within the active space and external excitations that involve at least one frozen orbital, $T_2 = T_2^{(\text{int})} + T_2^{(\text{ext})}$. Fixing the $T_2^{(\text{ext})}$ amplitudes to their MP2 values via Eq. (3), the downfolding method involves first solving Eqs. (4) for *only* the internal amplitudes and then evaluating the correlation energy expression Eq. (2) using *both* the internal and external amplitudes. Compared to the $O(N^2 M^4)$ cost of full CCD, the composite approach has $O(N^2 M_{\text{act}}^4) + O(N^2 M^2)$ cost and the downfolding approach has $O(N^2 M_{\text{act}}^2 M^2)$ cost, which can provide significant savings, depending on the practical value of the ratio M_{act}/M .

Let us now provide more insight into the “downfolding” perspective. Note that, because the internal and external excitation operators commute, the defining energy and amplitude equations of the downfolding approach can also be written

$$\begin{aligned} E_c &= \langle \Phi | e^{-T_2^{(\text{int})}} (\bar{H} - E_{\text{HF}}) e^{T_2^{(\text{int})}} | \Phi \rangle \\ &= E_{\text{MP2}}^{(\text{ext})} + \frac{1}{4} \sum_{ijab}^{\text{active}} t_{ij}^{ab} \langle ij || ab \rangle \end{aligned} \quad (5a)$$

$$0 = \langle \Phi | e^{-T_2^{(\text{int})}} \bar{H} e^{T_2^{(\text{int})}} | \Phi \rangle \quad (i, j, a, b) \text{ active} \quad (5b)$$

where $\bar{H} = e^{-T_2^{(\text{ext})}} H e^{T_2^{(\text{ext})}}$ (with fixed $T_2^{(\text{ext})}$ as detailed above) and $E_{\text{MP2}}^{(\text{ext})} = \frac{1}{4} \sum_{ijab}^{\text{active}} t_{ij}^{ab} \langle ij || ab \rangle$ is the MP2 correlation energy due to external excitations. These resemble ordinary CCD energy and amplitude equations *within the active space only*, except that the bare Hamiltonian H is replaced by an *effective* Hamiltonian \bar{H} that is similarity-transformed by the external excitation amplitudes. The effective Hamiltonian within the active space can be expressed as

$$\begin{aligned} \bar{H} - E_{\text{HF}} &= E_{\text{MP2}}^{(\text{ext})} + \sum_{pq}^{\text{active}} F_{pq} \{ a_p^\dagger a_q \} \\ &+ \frac{1}{4} \sum_{pqrs}^{\text{active}} W_{pqrs} \{ a_p^\dagger a_q^\dagger a_s a_r \} + \dots, \end{aligned} \quad (6)$$

where $\{ \dots \}$ indicates normal ordering of the operators. This effective Hamiltonian can be seen to contain effective one- and two-body interactions that are frequency independent,²¹ in contrast to other downfolding approaches like the constrained random-phase approximation.^{68,69} For example, the all-occupied two-body interaction becomes

$$W_{ijkl} = \langle ij || kl \rangle + \frac{1}{2} \sum_{ab}' \frac{\langle ij || ab \rangle \langle ab || kl \rangle}{\varepsilon_k + \varepsilon_l - \varepsilon_a - \varepsilon_b}, \quad (7)$$

where the primed summation indicates that one or both of a, b are inactive virtual orbitals. The frequency independence can be understood because our observable is the total energy rather than a spectral function. To summarize, an approach that solves the internal CCD amplitude equations in the presence of frozen external amplitudes is equivalent to a CCD calculation in an active space of orbitals using an effective (downfolded) Hamiltonian that is similarity-transformed by the external excitation operator.

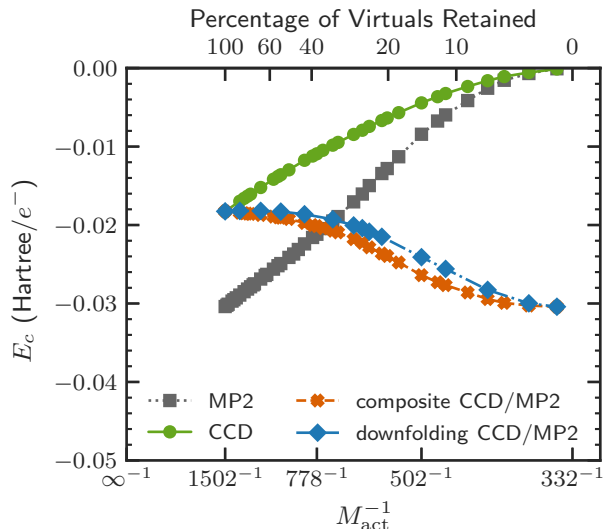


FIG. 1. Basis set convergence of the correlation energy of the $r_s = 4$ UEG with $N = 332$ electrons for MP2 (squares), CCD (circles), composite CCD/MP2 (crosses), and downfolding CCD/MP2 (diamonds). The top axis shows the percentage of virtual orbitals that are active for the composite and downfolding methods, compared to the “target” calculation with $M = 1502$. Both the composite and downfolding methods interpolate between the “target” MP2 calculation (leftmost square) and the “target” CCD calculation (leftmost circle).

It is straightforward to show that the composite approach, normally understood as a three-step procedure as shown in Eq. (1), is equivalent to Eqs. (5) but where the effective Hamiltonian \bar{H} is replaced by the bare Hamiltonian H in the amplitude equations (5b). From this perspective, the performance differences between the downfolding and composite approaches are attributable to the screening of the integrals in the effective Hamiltonian when determining the internal amplitudes. Nevertheless, we reiterate that the composite CCD/MP2 approach is expected to perform well because it replaces the problematic MP2 treatment of low-energy, internal double excitations with a well-behaved CCD treatment.

RESULTS AND DISCUSSION

We study the UEG as the simplest model of metals. A brief review of the UEG model in finite cells with finite plane-wave basis sets is given in the Appendix and we refer the reader to the literature for more details.^{31,40,70} To illustrate the performance of the composite and downfolding methods, we focus on the Wigner-Seitz radius $r_s = 4$ (corresponding to the approximate valence electron density of metallic sodium), where CCD has been found to recover about 85% of the correlation energy.^{40,43} We use a twisted boundary condition by performing calculations at the Baldereschi point,⁷¹ which has been shown to provide smoother convergence to the TDL.^{72,73}

In Fig. 1, we show basis set convergence of the correlation energy for a finite UEG with $N = 332$ electrons. The uncon-

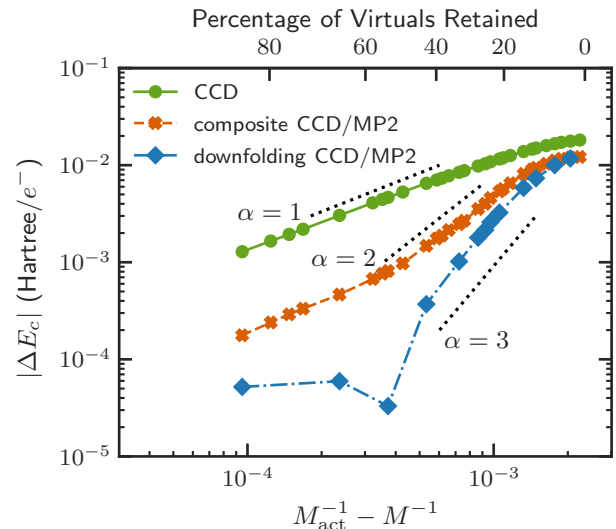


FIG. 2. Absolute error in the correlation energy for the data in Figure 1, shown on a logarithmic scale, relative to the “target” CCD result with $M = 1502$. The top axis and symbols have the same meaning as Figure 1. Dotted black lines are shown as a guide for various power law exponents α as discussed in the text.

rected MP2 and CCD correlation energies exhibit their typical slow convergence with increasing basis set size and show asymptotic behavior where the basis set error decays as M^{-1} . Extrapolation to the CBS limit yields $E_c/N = -0.0401 E_h$ for MP2 and $E_c/N = -0.0262 E_h$ for CCD. At the largest finite basis set shown, $M = 1502$, the results exhibit a significant basis set error of about $0.01 E_h$ for both methods, highlighting the challenge of recovering dynamical correlation in metals with large basis sets. Importantly, we emphasize that the MP2 correlation energy does not diverge for any finite system but only upon extrapolation to the TDL (see below).

Recall that the CCD/MP2 composite and downfolding approaches involve both a “target” number of orbitals M and an active number of orbitals M_{act} . In Fig. 1, we show results obtained for $M = 1502$ as M_{act} is varied. By construction, both methods yield the target MP2 correlation energy when there are no active virtual orbitals ($M_{\text{act}} = N$) and the target CCD correlation energy when all orbitals are active ($M_{\text{act}} = M$). We observe that both methods converge smoothly to the target CCD result and that the downfolding approach exhibits a faster convergence, due to its coupling between the internal and external excitation spaces. We also see similar behavior for other numbers of electrons and densities (not shown), indicating that neither finite-size effects nor the specific metallic density changes the overall picture.

To better quantify the rate of convergence, in Fig. 2 we plot the absolute deviation of the correlation energy from the “target” CCD result obtained with $M = 1502$. The error is plotted as a function of the difference between the inverse number of active orbitals and the inverse number of total orbitals and analyzed in terms of the power law $|\Delta E_c| \propto [M_{\text{act}}^{-1} - M^{-1}]^\alpha$. We compare the convergence of traditional CCD, the composite

approach, and the downfolding approach. For plain CCD, we see linear convergence of the correlation energy, with $\alpha \approx 1$, over a large range of basis set sizes. The composite method exhibits an early, rapid convergence reaching a maximum scaling of around $\alpha \approx 2$ before slowing to the same $\alpha \approx 1$ convergence as M_{act} approaches M . The rapid convergence for small M_{act} is responsible for absolute errors that are about one order of magnitude better than those obtained by simple truncation. In fact, the plain CCD result does not obtain mE_h accuracy until essentially all orbitals are correlated, whereas the composite result achieves this accuracy when only 50% of the virtual orbitals are correlated in the expensive CCD calculation; this results in a speedup of a factor of 16 compared to the full CCD calculation. Finally, the downfolding result exhibits rapid but non-monotonic convergence, making it difficult to extract a power law. Before slightly overshooting the “target”, the power law exponent reaches $\alpha \approx 3$ or better, a significant improvement over the composite CCD/MP2 and standard CCD approaches. This fast rate of convergence provides mE_h accuracy when about one third of the virtual orbitals are correlated, giving a speedup of a factor of 9.

The good performance of the composite approach indicates that MP2, while an inapplicable theory for three-dimensional metals, is safe to use for basis set corrections. As discussed above, the reason for this applicability can be understood by considering the MP2 correction that is applied in Eq. (1). This correction is a difference between two MP2 correlation energies, *both* of which correlate orbitals near the Fermi surface. These two MP2 energies are separately divergent in the TDL, but their difference is not; moreover, this difference is precisely $E_{\text{MP2}}^{\text{(ext)}}$ defined previously.

The reliable scaling of the MP2 basis set error at large M suggests that the MP2 CBS limit can be obtained by extrapolation for any given number of electrons. In contrast, the asymptotic scaling regime for the CCD correlation energy cannot always be reached. Thus, for any calculation performed with a given M , we propose to add the MP2 correlation energy difference $\delta^{(2)}(M) = E_{\text{MP2}}(\infty) - E_{\text{MP2}}(M)$, where $E_{\text{MP2}}(\infty)$ is obtained by M^{-1} extrapolation. Having obtained an estimate of the CBS limit for a given number of electrons, the finite-size extrapolation to the TDL can be done separately. We expect this scheme to be not only more reliable than extrapolating CCD on its own but also less costly since it involves more MP2 and fewer CCD calculations.

In Fig. 3(a), we plot the MP2 correlation energy as a function of the inverse number of electrons for finite UEG systems containing $N = 90$ –2392 electrons. For each system size, we performed MP2 calculations at different basis set sizes (grey squares), and the top four grey curves connect systems with a similar ratio of M/N . We then performed M^{-1} extrapolations at each particle number using data from $M/N \approx 3.0, 3.5, 4.0, 4.5$ to obtain the CBS limit at each system size (black stars). On approach to the TDL, the MP2 correlation energy diverges, as seen most easily in our largest calculations for the smaller values of M/N . Despite the divergence of its components, the MP2 CBS correction $\delta^{(2)}$, plotted explicitly in Fig. 3(a) for $M/N \approx 4$ (pink thin diamonds), does *not* diverge and is thus safe for use in metallic systems.

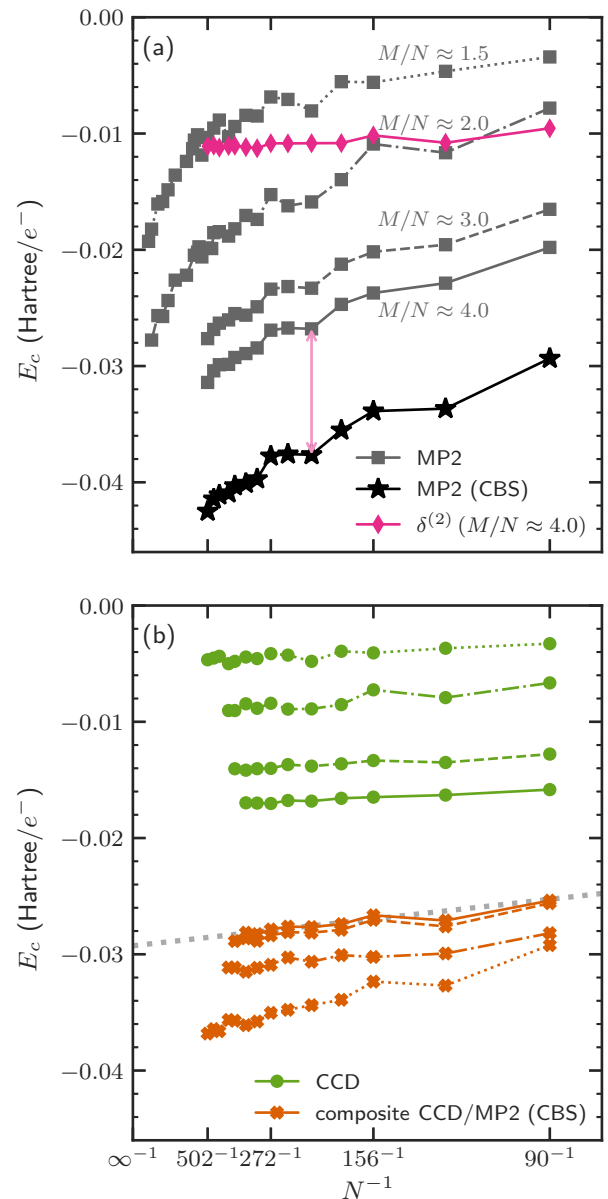


FIG. 3. Thermodynamic limit convergence of the correlation energy of the $r_s = 4$ UEG for systems with $N = 90$ –2392 electrons. (a) MP2 results for basis set sizes indicated (squares) and in the extrapolated CBS limit (stars). Thin diamonds show the CBS MP2 correction, $\delta^{(2)}(M/N \approx 4.0)$, indicated by the double-headed arrow at $N = 210$. (b) CCD (circles) and composite CCD/MP2 (crosses) results at the same (active) basis set sizes. For composite CCD/MP2, we applied the CBS MP2 correction $\delta^{(2)}(M)$. The grey line shows our TDL extrapolation using the largest five systems for $M/N \approx 4.0$.

To confirm that the success of the composite CCD/MP2 method holds on approach to the TDL, in Fig. 3(b) we plot results for CCD (green circles) and composite CCD/MP2 (orange crosses). For the composite CCD/MP2 result, we applied the MP2 CBS correction $\delta^{(2)}(M)$, although we note that a similar CBS correction could also be combined with the

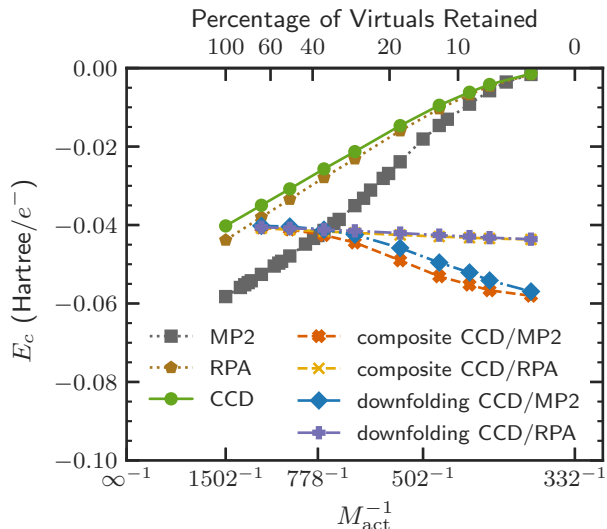


FIG. 4. The same as in Fig. 1, except for $r_s = 1$. In addition to the methods shown in Fig. 1, we also include RPA (pentagons), composite CCD/RPA (thin crosses), and downfolding CCD/RPA (pluses).

downfolding CCD/MP2 approach. In contrast to MP2, CCD is well-defined in the TDL; however, at each system size, convergence to the CBS limit is slow, as shown by the green data sets. In contrast, we observe that composite CCD/MP2 has much faster convergence to the TDL, as shown by the orange data sets. Performing a N^{-1} extrapolation of the CBS-corrected $M/N \approx 4.0$ results gives us a CBS and TDL extrapolated correlation energy of $E_c = -0.0293 E_h$, in general agreement with past CCD results.⁴⁰ For comparison, the exact value⁷⁴ is $E_c = -0.0318 E_h$, indicating that CCD recovers over 90% of the correlation energy. The same finite-size extrapolation of the CBS-corrected $M/N \approx 3.0$ data gives a correlation energy that differs by only $0.7 mE_h$, indicating the excellent convergence of the composite method.

Before concluding, we recognize that a variety of other low-level theories can be combined with CCD, in both the composite and downfolding manner. Of particular interest is the RPA, which is more appropriate for metals than MP2 but also more expensive. The so-called direct RPA is most promising computationally due to its low cost when two-electron integrals are handled by density fitting. Here we instead test the full particle-hole RPA, where the T_2 amplitudes maintain proper anti-symmetry so that the theory is free of self-interaction error. The RPA amplitudes are the solution of the CCD equations where only selected terms are retained.^{70,75} In Fig. 4, we show the same results as in Fig. 1, except for the electron density corresponding to $r_s = 1$ (due to RPA convergence problems at larger values of r_s ⁷⁰). We observe the same overall trends as we did at $r_s = 4$ for the MP2 and CCD calculations with finite basis sets. However, the RPA results follow the CCD results much more closely, which also makes composite and downfolding CCD/RPA significantly outperform the corresponding MP2 methods. Unsurprisingly, the improved performance of the downfolding approach compared to the com-

posite approach is even more marginal than for CCD/MP2.

CONCLUSIONS AND OUTLOOK

We have described and analyzed two approaches for eliminating basis set error in the CCD correlation energy of metals, using the simple UEG model. Our results indicate that these methods allow for aggressive freezing of virtual orbitals or approximation of external amplitudes, leading to significant reductions in computational cost. Although the downfolding CCD/MP2 approach is slightly more accurate, we find that the simpler composite CCD/MP2 approach is surprisingly effective because divergent contributions near the Fermi surface do not contribute to the basis set correction.

In this work, we have addressed post-Hartree-Fock basis set errors in the canonical orbital basis, but the methods we presented could also be straightforwardly applied in a basis of localized orbitals. For example, Refs. 57 and 76 used CCSD/MP2 and CCSD/RPA composite approaches to mitigate basis set errors in quantum embedding calculations. Localized orbital basis sets mix orbitals near and far from the Fermi surface, so it will be interesting to test how the composite and downfolding approaches perform when using these localized orbitals for metals.

Future work will focus on applying these techniques to atomistic metals using natural orbitals,⁷⁷ to the excited-state properties of metals,^{41,44} and to higher-level theories of correlation.⁴³ For example, we imagine that a composite CCSDT/CCSD or CCSDT/CCSD(T) approach would provide quantitative accuracy for metals while precluding the failure³¹ of the otherwise successful treatment of perturbative triple excitations.

ACKNOWLEDGMENTS

We thank Verena Neufeld and Sandeep Sharma for comments on the manuscript. This work was supported in part by the National Science Foundation Graduate Research Fellowship under Grant No. DGE-1644869 (M.F.L.), by the Department of Defense through the National Defense Science & Engineering Graduate (NDESG) Fellowship Program (J.M.C.), and by the National Science Foundation under Grant No. CHE-1848369 (T.C.B.). We acknowledge computing resources from Columbia University's Shared Research Computing Facility project, which is supported by NIH Research Facility Improvement Grant 1G20RR030893-01, and associated funds from the New York State Empire State Development, Division of Science Technology and Innovation (NYS-TAR) Contract C090171, both awarded April 15, 2010. The Flatiron Institute is a division of the Simons Foundation.

APPENDIX: UNIFORM ELECTRON GAS

Working in a single-particle basis of plane waves with momenta $\mathbf{k} = (2\pi/L)(n_x, n_y, n_z)$ and cell of volume L^3 with peri-

odic boundary conditions, the UEG Hamiltonian is given by

$$H = \sum_{\mathbf{k}\sigma} \frac{k^2}{2} a_{\mathbf{k}\sigma}^\dagger a_{\mathbf{k}\sigma} + \frac{1}{2} \sum_{\mathbf{k}_1 \mathbf{k}_2 \mathbf{k}_3 \mathbf{k}_4} \sum_{\sigma \sigma'} \langle \mathbf{k}_1 \sigma, \mathbf{k}_2 \sigma' | \mathbf{k}_3 \sigma, \mathbf{k}_4 \sigma' \rangle a_{\mathbf{k}_1 \sigma}^\dagger a_{\mathbf{k}_2 \sigma'}^\dagger a_{\mathbf{k}_4 \sigma'} a_{\mathbf{k}_3 \sigma} \quad (8)$$

where the primed summation requires $\mathbf{k}_1 + \mathbf{k}_2 = \mathbf{k}_3 + \mathbf{k}_4$. The two-electron repulsion integrals are given by

$$\langle \mathbf{k}_1 \sigma, \mathbf{k}_2 \sigma' | \mathbf{k}_3 \sigma, \mathbf{k}_4 \sigma' \rangle = v(\mathbf{k}_1 - \mathbf{k}_3) \delta_{\mathbf{k}_1 + \mathbf{k}_2, \mathbf{k}_3 + \mathbf{k}_4} \quad (9)$$

where the Ewald potential is

$$v(\mathbf{k}) = \begin{cases} \frac{4\pi}{L^3 k^2} & k \neq 0 \\ v_M & k = 0, \end{cases} \quad (10)$$

and $v_M = 2.837297479/L$ is the Madelung constant of the cell.⁷⁸ The N -electron reference determinant has the lowest-energy $N/2$ plane wave orbitals doubly occupied and the HF orbital energies are given by $\varepsilon(\mathbf{k}) = k^2/2 - v_M \theta(k_F - k)$, where k_F is the Fermi momentum. We restrict our calculations to closed-shell configurations, which allows only certain “magic numbers” of electrons and orbitals. At the Baldereschi point, the first few magic numbers are 2, 8, 14, 22, 34, 40, 52.

DATA AVAILABILITY STATEMENT

The data that support the findings of this study are available from the corresponding author upon reasonable request.

- ¹W. Kohn and L. J. Sham, “Self-consistent equations including exchange and correlation effects,” *Phys. Rev.* **140**, A1133–A1138 (1965).
- ²G. Kresse and J. Furthmüller, “Efficiency of ab-initio total energy calculations for metals and semiconductors using a plane-wave basis set,” *Comput. Mater. Sci.* **6**, 15–50 (1996).
- ³K. Burke, “Perspective on density functional theory,” *J. Chem. Phys.* **136**, 150901 (2012).
- ⁴R. O. Jones, “Density functional theory: Its origins, rise to prominence, and future,” *Rev. Mod. Phys.* **87**, 897–923 (2015).
- ⁵D. M. Ceperley and B. J. Alder, “Ground state of the electron gas by a stochastic method,” *Phys. Rev. Lett.* **45**, 566–569 (1980).
- ⁶P. Huang and E. A. Carter, “Advances in Correlated Electronic Structure Methods for Solids, Surfaces, and Nanostructures,” *Annu. Rev. Phys. Chem.* **59**, 261–290 (2008).
- ⁷G. Giuliani and G. Vignale, *Quantum theory of the electron liquid*, 1st ed. (Cambridge University Press, 2005).
- ⁸P. F. Loos and P. M. Gill, “The uniform electron gas,” *WIREs Comput. Mol. Sci.* **6**, 410–429 (2016).
- ⁹C. Pisani, L. Maschio, S. Casassa, M. Halo, M. Schütz, and D. Usvyat, “Periodic local MP2 method for the study of electronic correlation in crystals: Theory and preliminary applications,” *J. Comput. Chem.* **29**, 2113–2124 (2008).
- ¹⁰A. Grüneis, M. Marsman, and G. Kresse, “Second-order Møller-Plesset perturbation theory applied to extended systems. II. Structural and energetic properties,” *J. Chem. Phys.* **133**, 074107 (2010).
- ¹¹J. J. Shepherd, A. Grüneis, G. H. Booth, G. Kresse, and A. Alavi, “Convergence of many-body wave-function expansions using a plane-wave basis: From homogeneous electron gas to solid state systems,” *Phys. Rev. B* **86**, 035111 (2012).

- ¹²G. H. Booth, A. Grüneis, G. Kresse, and A. Alavi, “Towards an exact description of electronic wavefunctions in real solids,” *Nature* **493**, 365–370 (2013).
- ¹³J. Yang, W. Hu, D. Usvyat, D. Matthews, M. Schütz, and G. K.-L. Chan, “Ab initio determination of the crystalline benzene lattice energy to sub-kilojoule/mole accuracy,” *Science* **345**, 640–643 (2014).
- ¹⁴J. McClain, Q. Sun, G. K. L. Chan, and T. C. Berkelbach, “Gaussian-Based Coupled-Cluster Theory for the Ground-State and Band Structure of Solids,” *J. Chem. Theory Comput.* **13**, 1209–1218 (2017).
- ¹⁵T. Gruber, K. Liao, T. Tsatsoulis, F. Hummel, and A. Grüneis, “Applying the Coupled-Cluster Ansatz to Solids and Surfaces in the Thermodynamic Limit,” *Phys. Rev. X* **8**, 021043 (2018).
- ¹⁶J. G. Brandenburg, A. Zen, M. Fitzner, B. Ramberger, G. Kresse, T. Tsatsoulis, A. Grüneis, A. Michaelides, and D. Alfè, “Physisorption of Water on Graphene: Subchemical Accuracy from Many-Body Electronic Structure Methods,” *J. Phys. Chem. Lett.* **10**, 358–368 (2019).
- ¹⁷T. Tsatsoulis, F. Hummel, D. Usvyat, M. Schütz, G. H. Booth, S. S. Binnie, M. J. Gillan, D. Alfè, A. Michaelides, and A. Grüneis, “A comparison between quantum chemistry and quantum Monte Carlo techniques for the adsorption of water on the (001) LiH surface,” *J. Chem. Phys.* **146**, 204108 (2017).
- ¹⁸D. Usvyat, L. Maschio, and M. Schütz, “Periodic and fragment models based on the local correlation approach,” *WIREs Comput. Mol. Sci.* **8**, e1357 (2018).
- ¹⁹J. Harl and G. Kresse, “Accurate Bulk Properties from Approximate Many-Body Techniques,” *Phys. Rev. Lett.* **103**, 056401 (2009).
- ²⁰A. Grüneis, M. Marsman, J. Harl, L. Schimka, and G. Kresse, “Making the random phase approximation to electronic correlation accurate,” *J. Chem. Phys.* **131** (2009), 10.1063/1.3250347.
- ²¹I. Shavitt and R. J. Bartlett, *Many-body methods in chemistry and physics: MBPT and coupled cluster theory* (Cambridge University Press, Cambridge, 2009).
- ²²R. J. Bartlett, “Coupled-cluster theory and its equation-of-motion extensions,” *WIREs Comput. Mol. Sci.* **2**, 126–138 (2012).
- ²³I. Y. Zhang and A. Grüneis, “Coupled cluster theory in materials science,” *Front. Mater.* **6**, 123 (2019).
- ²⁴A. Grüneis, “Coupled Cluster and Quantum Chemistry Schemes for Solids,” in *Handbook of Materials Modeling* (Springer International Publishing, Cham, 2020) pp. 453–468.
- ²⁵H. Stoll, B. Paulus, and P. Fulde, “An incremental coupled-cluster approach to metallic lithium,” *Chem. Phys. Lett.* **469**, 90–93 (2009).
- ²⁶F. Hummel, “Finite Temperature Coupled Cluster Theories for Extended Systems,” *J. Chem. Theory Comput.* **14**, 6505–6514 (2018).
- ²⁷M. Gell-Mann and K. A. Brueckner, “Correlation energy of an electron gas at high density,” *Phys. Rev.* **106**, 364–368 (1957).
- ²⁸D. Bohm, K. Huang, and D. Pines, “Role of Subsidiary Conditions in the Collective Description of Electron Interactions,” *Phys. Rev.* **107**, 71–80 (1957).
- ²⁹D. L. Freeman, “Coupled-cluster expansion applied to the electron gas: Inclusion of ring and exchange effects,” *Phys. Rev. B* **15**, 5512–5521 (1977).
- ³⁰R. J. Bartlett and M. Musiał, “Coupled-cluster theory in quantum chemistry,” *Rev. Mod. Phys.* **79**, 291–352 (2007).
- ³¹J. J. Shepherd and A. Grüneis, “Many-body quantum chemistry for the electron gas: Convergent perturbative theories,” *Phys. Rev. Lett.* **110**, 226401 (2013).
- ³²K. Liao and A. Grüneis, “Communication: Finite size correction in periodic coupled cluster theory calculations of solids,” *J. Chem. Phys.* **145**, 141102 (2016).
- ³³T. Gruber and A. Grüneis, “Ab initio calculations of carbon and boron nitride allotropes and their structural phase transitions using periodic coupled cluster theory,” *Phys. Rev. B* **98**, 134108 (2018).
- ³⁴A. Dittmer, R. Izsák, F. Neese, and D. Maganas, “Accurate Band Gap Predictions of Semiconductors in the Framework of the Similarity Transformed Equation of Motion Coupled Cluster Theory,” *Inorg. Chem.* **58**, 9303–9315 (2019).
- ³⁵Y. Gao, Q. Sun, J. M. Yu, M. Motta, J. McClain, A. F. White, A. J. Minnich, and G. K. L. Chan, “Electronic structure of bulk manganese oxide and nickel oxide from coupled cluster theory,” *Phys. Rev. B* **101**, 165138 (2020).
- ³⁶X. Wang and T. C. Berkelbach, “Excitons in Solids from Periodic Equation-of-Motion Coupled-Cluster Theory,”

- J. Chem. Theory Comput.* **16**, 3095–3103 (2020).
- ³⁷A. Pulkin and G. K. L. Chan, “First-principles coupled cluster theory of the electronic spectrum of transition metal dichalcogenides,” *Phys. Rev. B* **101**, 241113 (2020).
- ³⁸D. L. Freeman, “Application of the coupled-cluster expansion to the correlation energy of electrons in two-dimensional and quasi-two-dimensional systems,” *Solid State Commun.* **26**, 289–293 (1978).
- ³⁹D. L. Freeman, “Coupled-cluster summation of the particle-particle ladder diagrams for the two-dimensional electron gas,” *J. Phys. C Solid State* **16**, 711–727 (1983).
- ⁴⁰J. J. Shepherd, “Communication: Convergence of many-body wavefunction expansions using a plane-wave basis in the thermodynamic limit,” *J. Chem. Phys.* **145**, 031104 (2016).
- ⁴¹J. McClain, J. Lischner, T. Watson, D. A. Matthews, E. Ronca, S. G. Louie, T. C. Berkelbach, and G. K. L. Chan, “Spectral functions of the uniform electron gas via coupled-cluster theory and comparison to the GW and related approximations,” *Phys. Rev. B* **93**, 235139 (2016).
- ⁴²J. S. Spencer and A. J. W. Thom, “Developments in stochastic coupled cluster theory: The initiator approximation and application to the uniform electron gas,” *J. Chem. Phys.* **144**, 084108 (2016).
- ⁴³V. A. Neufeld and A. J. Thom, “A study of the dense uniform electron gas with high orders of coupled cluster,” *J. Chem. Phys.* **147**, 194105 (2017).
- ⁴⁴A. M. Lewis and T. C. Berkelbach, “Ab Initio Lifetime and Concomitant Double-Excitation Character of Plasmons at Metallic Densities,” *Phys. Rev. Lett.* **122**, 226402 (2019).
- ⁴⁵A. F. White and G. Kin-Lic Chan, “Finite-temperature coupled cluster: Efficient implementation and application to prototypical systems,” *J. Chem. Phys.* **152**, 224104 (2020).
- ⁴⁶J. J. Shepherd, G. Booth, A. Grüneis, and A. Alavi, “Full configuration interaction perspective on the homogeneous electron gas,” *Phys. Rev. B* **85**, 081103 (2012).
- ⁴⁷C. Hättig, W. Klopper, A. Köhn, and D. P. Tew, “Explicitly Correlated Electrons in Molecules,” *Chem. Rev.* **112**, 4–74 (2012).
- ⁴⁸A. Grüneis, J. J. Shepherd, A. Alavi, D. P. Tew, and G. H. Booth, “Explicitly correlated plane waves: Accelerating convergence in periodic wavefunction expansions,” *J. Chem. Phys.* **139**, 084112 (2013).
- ⁴⁹H. Luo and A. Alavi, “Combining the Transcorrelated Method with Full Configuration Interaction Quantum Monte Carlo: Application to the Homogeneous Electron Gas,” *J. Chem. Theory Comput.* **14**, 1403–1411 (2018).
- ⁵⁰K. Liao, T. Schraivogel, H. Luo, D. Kats, and A. Alavi, “Towards efficient and accurate ab initio solutions to periodic systems via transcorrelation and coupled cluster theory,” [arXiv:2103.03176](https://arxiv.org/abs/2103.03176).
- ⁵¹B. Fiedler, G. Schmitz, C. Hättig, and J. Friedrich, “Combining Accuracy and Efficiency: An Incremental Focal-Point Method Based on Pair Natural Orbitals,” *J. Chem. Theory Comput.* **13**, 6023–6042 (2017).
- ⁵²A. Kumar and T. D. Crawford, “Frozen Virtual Natural Orbitals for Coupled-Cluster Linear-Response Theory,” *J. Phys. Chem. A* **121**, 708–716 (2017).
- ⁵³C. E. Warden, D. G. A. Smith, L. A. Burns, U. Bozkaya, and C. D. Sherrill, “Efficient and automated computation of accurate molecular geometries using focal-point approximations to large-basis coupled-cluster theory,” *J. Chem. Phys.* **152**, 124109 (2020).
- ⁵⁴A. Irmmler, A. Gallo, F. Hummel, and A. Grüneis, “Duality of Ring and Ladder Diagrams and Its Importance for Many-Electron Perturbation Theories,” *Phys. Rev. Lett.* **123**, 156401 (2019).
- ⁵⁵A. Irmmler and A. Grüneis, “Particle-particle ladder based basis-set corrections applied to atoms and molecules using coupled-cluster theory,” *J. Chem. Phys.* **151**, 104107 (2019).
- ⁵⁶M. F. Lange and T. C. Berkelbach, “Active space approaches combining coupled-cluster and perturbation theory for ground states and excited states,” *Mol. Phys.* **118**, e1808726 (2020).
- ⁵⁷B. T. G. Lau, G. Knizia, and T. C. Berkelbach, “Regional Embedding Enables High-Level Quantum Chemistry for Surface Science,” *J. Phys. Chem. Lett.* **12**, 1104–1109 (2021).
- ⁵⁸T. Kinoshita, O. Hino, and R. J. Bartlett, “Coupled-cluster method tailored by configuration interaction,” *J. Chem. Phys.* **123**, 074106 (2005).
- ⁵⁹P. Piecuch, S. A. Kucharski, and V. Špirko, “Coupled-cluster methods with internal and semi-internal triply excited clusters: Vibrational spectrum of the HF molecule,” *J. Chem. Phys.* **111**, 6679–6692 (1999).
- ⁶⁰K. Kowalski and P. Piecuch, “The state-universal multi-reference coupled-cluster theory with perturbative description of core–virtual excitations,” *Chem. Phys. Lett.* **334**, 89–98 (2001).
- ⁶¹P. Piecuch, “Active-space coupled-cluster methods,” *Mol. Phys.* **108**, 2987–3015 (2010).
- ⁶²J. Shen and P. Piecuch, “Combining active-space coupled-cluster methods with moment energy corrections via the CC(P;Q) methodology, with benchmark calculations for biradical transition states,” *J. Chem. Phys.* **136**, 144104 (2012).
- ⁶³A. K. Dutta, M. Nooijen, F. Neese, and R. Izsák, “Automatic active space selection for the similarity transformed equations of motion coupled cluster method,” *J. Chem. Phys.* **146**, 074103 (2017).
- ⁶⁴M. Nooijen, “Combining coupled cluster and perturbation theory,” *J. Chem. Phys.* **111**, 10815–10826 (1999).
- ⁶⁵A. D. Bochevarov and C. D. Sherrill, “Hybrid correlation models based on active-space partitioning: Correcting second-order Møller-Plesset perturbation theory for bond-breaking reactions,” *J. Chem. Phys.* **122**, 234110 (2005).
- ⁶⁶R. H. Myhre, A. M. Sánchez De Merás, and H. Koch, “The extended CC2 model ECC2,” *Mol. Phys.* **111**, 1109–1118 (2013).
- ⁶⁷R. H. Myhre, A. M. J. Sánchez de Merás, and H. Koch, “Multi-level coupled cluster theory,” *J. Chem. Phys.* **141**, 224105 (2014).
- ⁶⁸F. Aryasetiawan, M. Imada, A. Georges, G. Kotliar, S. Biermann, and A. I. Lichtenstein, “Frequency-dependent local interactions and low-energy effective models from electronic structure calculations,” *Phys. Rev. B* **70**, 195104 (2004).
- ⁶⁹T. Miyake and F. Aryasetiawan, “Screened Coulomb interaction in the maximally localized Wannier basis,” *Phys. Rev. B* **77**, 085122 (2008).
- ⁷⁰J. J. Shepherd, T. M. Henderson, and G. E. Scuseria, “Coupled cluster channels in the homogeneous electron gas,” *J. Chem. Phys.* **140**, 124102 (2014).
- ⁷¹A. Baldereschi, “Mean-value point in the Brillouin zone,” *Phys. Rev. B* **7**, 5212–5215 (1973).
- ⁷²N. D. Drummond, R. J. Needs, A. Sorouri, and W. M. Foulkes, “Finite-size errors in continuum quantum Monte Carlo calculations,” *Phys. Rev. B* **78**, 125106 (2008).
- ⁷³T. N. Mihm, A. R. McIsaac, and J. J. Shepherd, “An optimized twist angle to find the twist-averaged correlation energy applied to the uniform electron gas,” *J. Chem. Phys.* **150**, 191101 (2019).
- ⁷⁴S. H. Vosko, L. Wilk, and M. Nusair, “Accurate spin-dependent electron liquid correlation energies for local spin density calculations: a critical analysis,” *Can. J. Phys.* **58**, 1200–1211 (1980).
- ⁷⁵G. E. Scuseria, T. M. Henderson, and D. C. Sorensen, “The ground state correlation energy of the random phase approximation from a ring coupled cluster doubles approach,” *J. Chem. Phys.* **129**, 231101 (2008).
- ⁷⁶T. Schäfer, F. Libisch, G. Kresse, and A. Grüneis, “Local embedding of coupled cluster theory into the random phase approximation using plane waves,” *J. Chem. Phys.* **154**, 011101 (2021).
- ⁷⁷A. Grüneis, G. H. Booth, M. Marsman, J. Spencer, A. Alavi, and G. Kresse, “Natural Orbitals for Wave Function Based Correlated Calculations Using a Plane Wave Basis Set,” *J. Chem. Theory Comput.* **7**, 2780–2785 (2011).
- ⁷⁸C. A. Sholl, “The calculation of electrostatic energies of metals by plane-wave summation,” *Proc. Phys. Soc.* **92**, 434–445 (1967).